A Position Control Differential Drive Wheeled Mobile Robot

Yongoug Chung, Chongkug Park, *Member, IEEE*, and Fumio Harashima, *Fellow, IEEE*

***Abstract*—For more accurate path tracking of a four-wheeled two-degrees-of-freedom mobile robot (WMR), a position control algorithm is proposed with two separated feedback loops, a velocity feedback loop and a position feedback loop. In the most conventional position control system of a WMR, internal error is mainly considered, while external error has, as yet, hardly been treated, although it plays an important role in accurate position control. This external error is caused by unexpected environmental situations. The proposed control algorithm is designed to compensate for both internal error and external error. This algorithm makes it possible to accurately follow the designed trajectory.**

***Index Terms*—External error, internal error, kinematics, nonholonomic constraint, wheeled mobile robot.**

I. Introduction

ALTHOUGH recent research into mobile robots has progressed remarkably, there are still certain limits to accurate path tracking. Many efforts to improve such problems have been tried, and still go on by way of developing the controller of the system. In this paper, we propose a new type of controller of four-wheeled two-degrees-of-freedom mobile robots (WMRs), which has a good path tracking ability and can be easily adapted to the system.

In the conventional position control algorithm of the WMR, the output of the system, including the position and orientation sensing data, are feedback together to the system input through a feedback loop. Petrov [3] also used the same technique when he developed his robust path–tracking algorithm for a WMR. He considers both position and orientation in a trajectory. Kanayama [4] also used a similar technique when he suggested a stable path–tracking algorithm for a WMR.

In this paper, we suggest a more systematic kinematics, and propose a control algorithm that can compensate for both internal error and external error. Internal error occurs from inappropriate setting up of the parameters and the time constant. External error inevitably appears while a WMR is driving; it occurs by virtue of the two driving wheels' different friction and radius. To minimize such errors, we propose a feedback controller that has two separated feedback loops; one of which is a position feedback, and the other an orientation feedback. This controller computes the two driving wheels' velocity, and the difference of the two wheels' moving distance in a sampling time. Then, these are applied to the wheels' driving velocities to compensate for external errors.

To yield high performance and operability in real time, a dead–reckoning algorithm is added to this control loop. We pay more attention to minimum orientation error, because the most essential thing is to maintain accuracy while the robot runs. However, to get enhanced results in practical implementation, fusion data from external sensors can be considered.

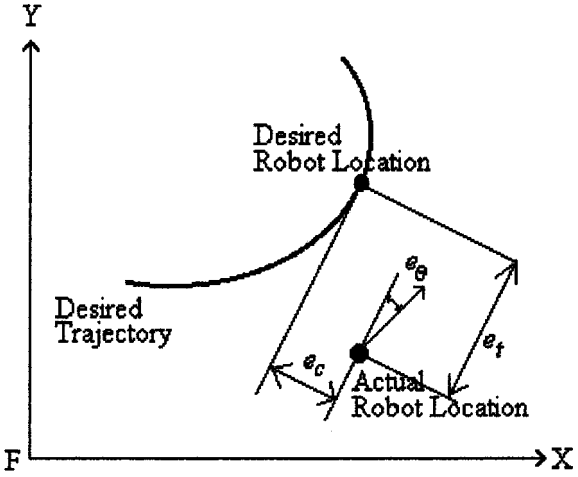

Fig. 1. Motion error decomposition.

II. Analysis of Motion Error of WMR

The motions of a WMR are classified as e_θ, e_c, and e_t as shown in Fig. 1. e_θ is orientation error, defined by the angle difference between real orientation and desired orientation. This is the most significant error because it results from superficial error, it also produces the biggest trouble while the system maintains motion accuracy. e_c is defined as the distance difference between the WMR's real position and desired position. e_t is tracking error, and is defined as the difference in distance between real position and desired position along the WMR's moving direction. Minimization of orientation error makes it possible for the WMR to move parallel to the desired path.

Manuscript received August 1, 2000; revised February 1, 2001. Abstract published on the Internet June 6, 2001.

Y. Chung is with the School of Automotive Engineering, Chinju College, Chinju City 660-759, Korea (e-mail: yochung@namgang.chinju-c.ac.kr).

C. Park is with the School of Electronics and Information, Kyung Hee University, Yongin-Shi 449-701, Korea (e-mail: ckpark@khu.ac.kr).

F. Harashima is with Tokyo Metropolitan Institute of Technology, Tokyo 191-0065, Japan (e-mail: f.harashima@tmit.ac.jp; f.harashima@ieee.org).

Publisher Item Identifier S 0278-0046(01)06288-8.

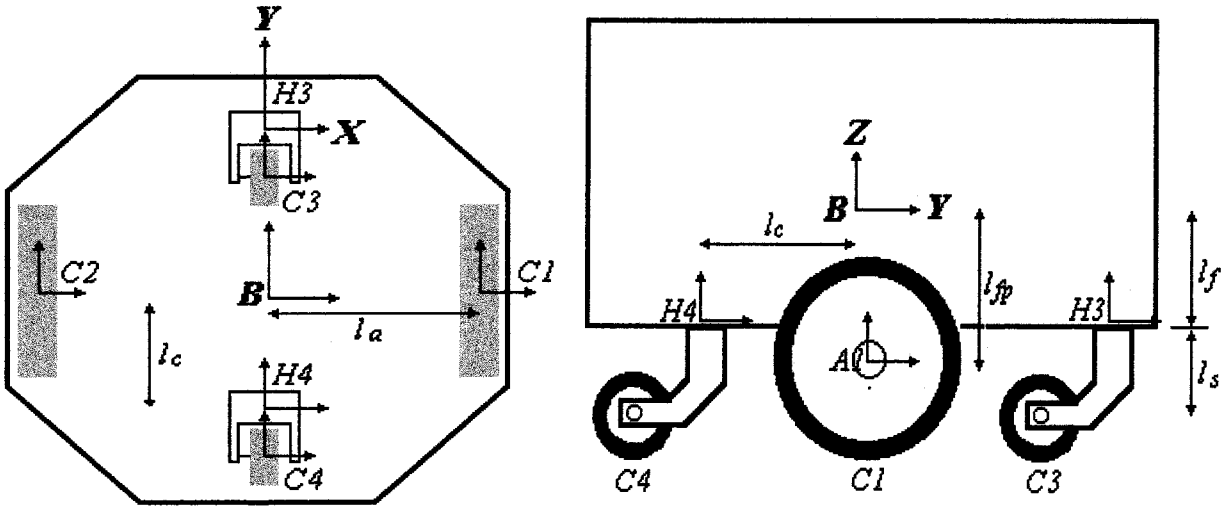

Fig. 2. Configurations of WMR.

III. Kinematic's Model

In the WMR, wheels 1 and 2 are driving wheels that are driven by separated actuator motors. Wheels 3 and 4 are casters. The geometrical characters of wheels 1, 2, 3, and 4 are as follows:

$$\begin{aligned}
&R1 = R,\ d_{c1y} = l_b = 0,\ d_{c1x} = l_a \\
\text{wheel 1:}\quad &\\
&\sin^B\theta_{c1z} = 0,\ \cos^B\theta_{c1z} = 1 \\
&R2 = R,\ d_{c2y} = l_b = 0,\ d_{c2x} = -l_a \\
\text{wheel 2:}\quad &\\
&\sin^B\theta_{c2z} = 0,\ \cos^B\theta_{c2z} = 1 \\
\text{wheel 3:}\quad &R3 = r,\ d_{c3y} = l_c,\ d_{c3x} = 0 \\
\text{wheel 4:}\quad &R4 = r,\ d_{c4y} = -l_c,\ d_{c4x} = 0.
\end{aligned}$$

Here, θ and d are the rotation angle and displacement for body reference coordinate (B). The kinematics are derived from the configuration of the robot shown in Fig. 2.

Three assumptions should be mentioned regarding the kinematics.

1) The wheeled mobile robot does not have flexible parts. The driving wheel has no steering link, or only one steering link.
2) The steering axial is perpendicular to the surface.
3) The mobile robot moves on a planar surface and does not have slippage.

The configuration of the WMR in three dimensions is shown in Fig. 3.

A. Solution of Actuated Inverse Kinematics

The actuated wheel velocity is derived from robot body velocity. To separate wheel parameter as an actuated component, and an unactuated component, the wheel equation is separated into two parts

$$^{\overline{B}}\dot{p}_B = J_{ia}\dot{q}_{ia} + J_{iu}\dot{q}_{iu}, \qquad \text{for } i = 1, 2. \tag{1}$$

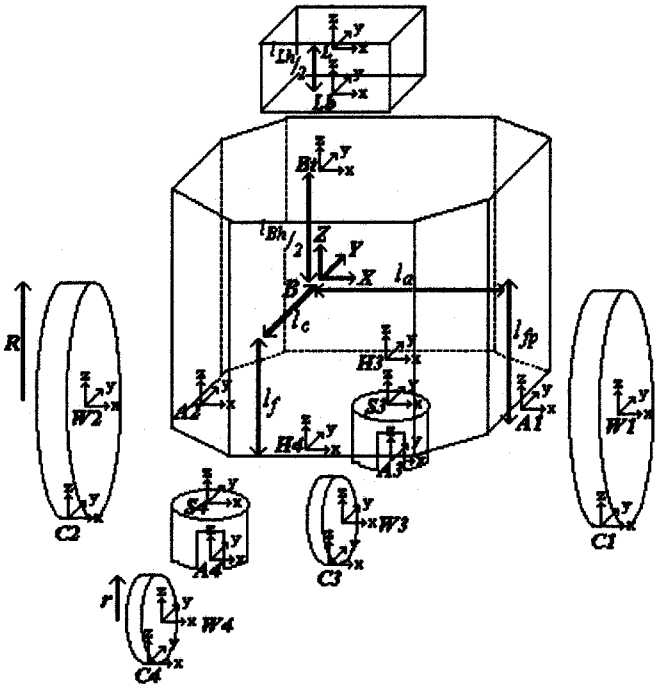

Fig. 3. Configuration of WMR in three dimensions.

Here "a" is the actuated component and "u" is the unactuated component. Also, subscript i represents wheel 1 and wheel 2, which are driven by independent driving motors.

If we combine these separated wheel equations, and use a wheel Jacobian matrix to derive an equation, then

$$\begin{bmatrix} I_1 \\ I_2 \end{bmatrix} {}^{\overline{B}}\dot{p}_B = \begin{bmatrix} 0 & 0 & 0 & 0 \\ R & 0 & -l_a & 0 \\ 0 & 0 & 1 & 0 \\ 0 & 0 & 0 & 0 \\ 0 & R & 0 & l_a \\ 0 & 0 & 0 & 1 \end{bmatrix} \begin{bmatrix} \omega_{w1x} \\ \omega_{w2x} \\ \omega_{c1z} \\ \omega_{c2z} \end{bmatrix} \tag{2}$$

or

$$A_0 {}^{\overline{B}}\dot{p}_B = B_{op}\begin{bmatrix}\dot{q}_a\\ \dot{q}_u\end{bmatrix}. \tag{3}$$

In (3), we have to use a pseudo-inverse matrix [6] to get a solution for $[\dot{q}_a \quad \dot{q}_u]^T$, because B_{op} is not a square matrix. Then, we can get an actuated inverse kinematic's equation as follows:

$$\begin{bmatrix}\omega_{w1x}\\ \omega_{w2x}\end{bmatrix} = \frac{1}{R}\begin{bmatrix}0 & 1 & l_a\\ 0 & 1 & -l_a\end{bmatrix}\begin{bmatrix}{}^{\overline{B}}v_{Bx}\\ {}^{\overline{B}}v_{By}\\ {}^{\overline{B}}\omega_{Bz}\end{bmatrix}. \tag{4}$$

In (4), we use motion matrix M to transform the trajectory description for robot coordinate B, into a description for the fixed reference coordinate F. When the WMR body velocity is applied to fixed reference coordinate F, then each wheel's angular velocity is derived as in (5). Equation (5) is a mathematical formula describing how the linear velocity and the angular velocity of a mobile robot, for body coordinate (B), are changed into that for fixed surface reference coordinate (F), by motion matrix M. Then, the linear velocity of the mobile robot, for fixed surface reference coordinate (F), is changed again by the angular velocity of driving wheels 1 and 2, through transfer matrix

$$\begin{bmatrix}{}^{F}v_{Bx}\\ {}^{F}v_{By}\\ {}^{F}\omega_{Bz}\end{bmatrix} = M\begin{bmatrix}{}^{\overline{B}}v_{Bx}\\ {}^{\overline{B}}v_{By}\\ {}^{\overline{B}}\omega_{Bz}\end{bmatrix} = \begin{bmatrix}C\theta & -S\theta & 0\\ S\theta & C\theta & 0\\ 0 & 0 & 1\end{bmatrix}\begin{bmatrix}{}^{\overline{B}}v_{Bx}\\ {}^{\overline{B}}v_{By}\\ {}^{\overline{B}}\omega_{Bz}\end{bmatrix}$$

$$\begin{bmatrix}\omega_{w1x}\\ \omega_{w2x}\end{bmatrix} = \frac{1}{R}\begin{bmatrix}-S\theta & C\theta & l_a\\ -S\theta & C\theta & -l_a\end{bmatrix}\begin{bmatrix}{}^{F}v_{Bx}\\ {}^{F}v_{By}\\ {}^{F}\omega_{Bz}\end{bmatrix}. \tag{5}$$

B. Solution of Sensed Forward Kinematics

Robot velocity vector ${}^{\overline{B}}\dot{p}_B$ can be derived from wheel position q_s and velocity $\dot{q}_s$. For the first step of deriving the forward kinematic's solution, we separate the velocity as sensed part and not sensed part, by denoting subscripts s and n. Then, we get

$$\begin{aligned}{}^{\overline{B}}\dot{p}_B &= J_{is}\dot{q}_{is} + J_{in}\dot{q}_{in} \qquad \text{for } i = 1, 2\\ &= \begin{bmatrix}0 & 0\\ R & 0\\ 0 & 0\\ 0 & 0\\ 0 & R\\ 0 & 0\end{bmatrix}\begin{bmatrix}\omega_{w1x}\\ \omega_{w2x}\end{bmatrix} + \begin{bmatrix}0 & 0\\ -l_a & 0\\ 1 & 0\\ 0 & 0\\ 0 & l_a\\ 0 & 1\end{bmatrix}\begin{bmatrix}\omega_{c1z}\\ \omega_{c2z}\end{bmatrix}.\end{aligned} \tag{6}$$

From (6), the solution for sensed forward kinematics can be derived as follows:

$$\begin{bmatrix}{}^{\overline{B}}v_{Bx}\\ {}^{\overline{B}}v_{By}\\ {}^{\overline{B}}\omega_{Bz}\end{bmatrix} = \frac{R}{2l_a}\begin{bmatrix}0 & 0\\ l_a & l_a\\ 1 & -1\end{bmatrix}\begin{bmatrix}\omega_{w1x}\\ \omega_{w2x}\end{bmatrix}. \tag{7}$$

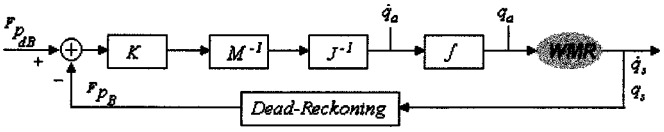

Fig. 4. Conventional feedback control system.

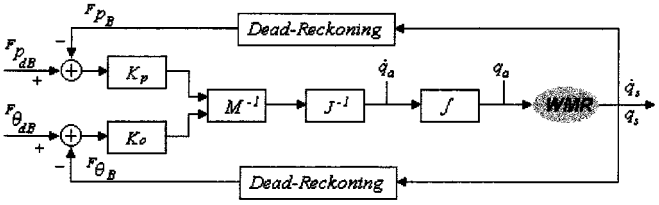

Fig. 5. Position-orientation feedback control system.

If we apply wheel motion matrix M to (7), in order to derive a robot body velocity for fixed reference coordinate F, then we can get (8)

$$\begin{aligned}\begin{bmatrix}{}^{F}v_{Bx}\\ {}^{F}v_{By}\\ {}^{F}\omega_{Bz}\end{bmatrix} &= M\begin{bmatrix}{}^{\overline{B}}v_{Bx}\\ {}^{\overline{B}}v_{By}\\ {}^{\overline{B}}\omega_{Bz}\end{bmatrix}\\ &= \frac{R}{2l_a}\begin{bmatrix}C\theta & -S\theta & 0\\ S\theta & C\theta & 0\\ 0 & 0 & 1\end{bmatrix}\begin{bmatrix}0 & 0\\ l_a & l_a\\ 1 & -1\end{bmatrix}\begin{bmatrix}\omega_{w1x}\\ \omega_{w2x}\end{bmatrix}\\ &= \frac{R}{2l_a}\begin{bmatrix}-l_aS\theta & -l_aS\theta\\ l_aC\theta & l_aC\theta\\ 1 & -1\end{bmatrix}\begin{bmatrix}\omega_{w1x}\\ \omega_{w2x}\end{bmatrix}.\end{aligned} \tag{8}$$

IV. Feedback Control System for Position Control

A. Conventional Control System

In conventional control systems for differential mobile robots, a feedback loop that has both position and orientation is used, [3] and [4]. Fig. 4 shows such a conventional feedback control system.

Wheel position $q_s(nT)$ and velocity $\dot{q}_s(nT)$ at time nT are derived from the feedback data of shaft encoders, and the desired robot position vector ${}^{F}p_d(nT)$. To find out robot position ${}^{F}p_d(nT)$, we apply a dead–reckoning algorithm [2], which gives us (9).

As shown in Fig. 4, the definition of ${}^{F}e_B(nT)$ in (9) is a trajectory error matrix that is obtained from the difference between reference trajectory ${}^{F}P_{dB}(nT)$, and solution trajectory ${}^{F}P_B(nT)$. This is obtained through dead reckoning. We appended an amplificative explanation of it in (9). Equation (9) is a formula that derives the updated angular velocity

$$\begin{aligned}&{}^{F}p_d(nT)\begin{bmatrix}\omega_{w1x}(nt)\\ \omega_{w2x}(nt)\end{bmatrix}\\ &\quad = \frac{1}{R}\begin{bmatrix}-S^{F}\theta_{Bz}(nt)K_x & C^{F}\theta_{Bz}(nt)K_y & l_aK_z\\ -S^{F}\theta_{Bz}(nt)K_x & C^{F}\theta_{Bz}(nt)K_y & -l_aK_z\end{bmatrix}\\ &\quad\quad \cdot {}^{F}e_B(nt).\end{aligned} \tag{9}$$

B. Position-Orientation Feedback Control System

In conventional feedback control systems, both sensed data of position, and orientation, are feedback to system input through

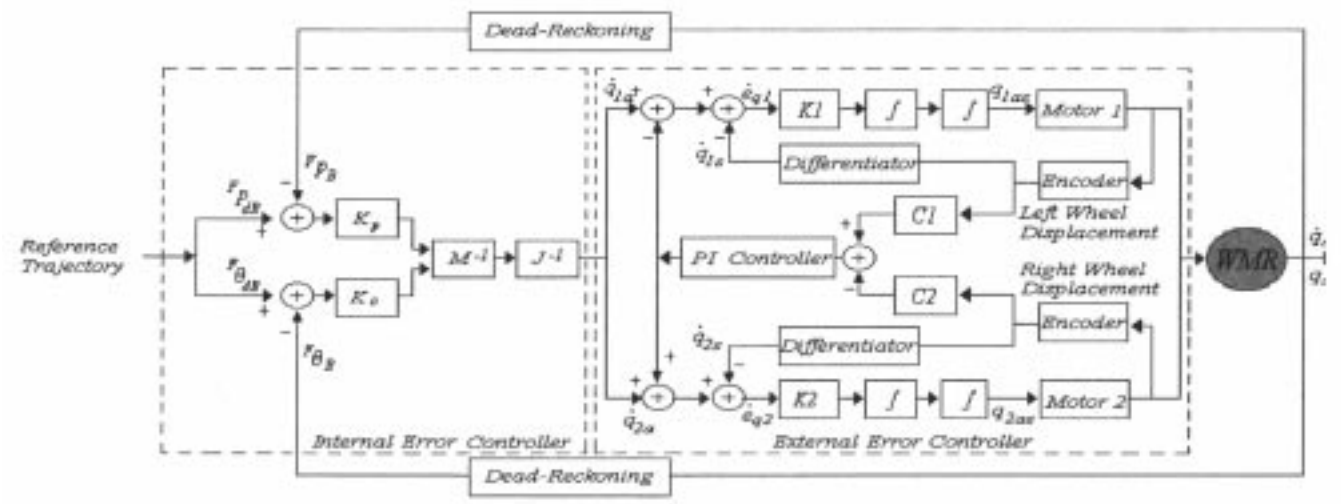

Fig. 6. Proposed control system.

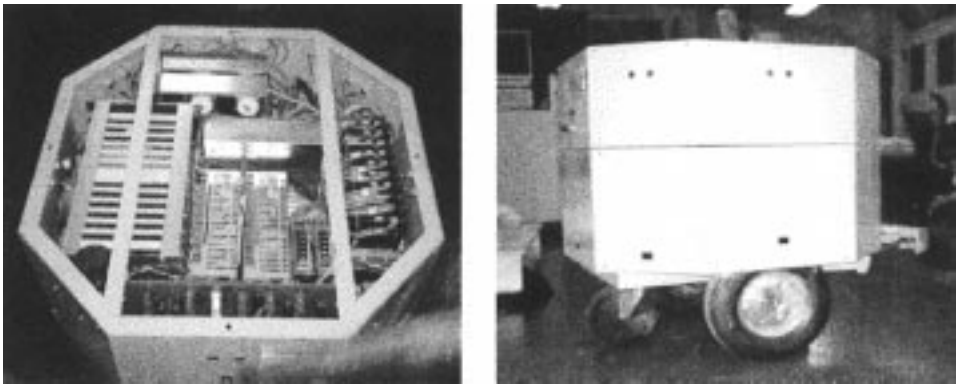

Fig. 7. Configuration of WMR.

TABLE I
PARAMETER VALUES OF WMR

Notation	Numerical value	Unit	Meaning
$l_{Lb}/2$	0.25	M	Load Height/2
$l_{Bb}/2$	0.3	M	Body Height/2
L_a	0.32	M	Body Width/2
L_c	0.32	M	Caster y-displacement
L_f	0.22	M	Caster z-displacement
l_{fp}	0.24	M	Caster z-displacement
L_e	0.1	M	Caster Height
L_g	0.02	M	Caster's Length of Steering
R1	0.11	M	Left Driving Wheel's Radius
R2	0.11	M	Right Driving Wheel's Radius
R	0.03	M	Caster Radius

a feedback loop. However, in our proposed feedback control system, wheel velocity, and position sensed by shaft encoders, are feedback to desired inputs of position and velocity, respectively. Therefore, they minimize the error of position and orientation, by pertinent selection of position gain matrix K_p and orientation gain matrix K_o.

Namely, position and orientation errors are obtained by separated position and orientation feedback. The mobile robot's linear

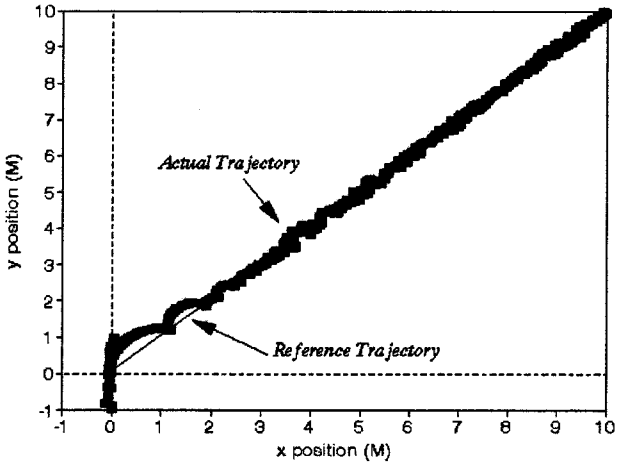

(a)

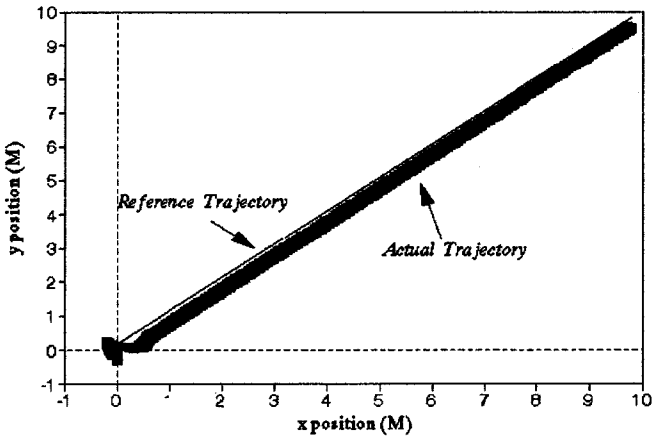

(b)

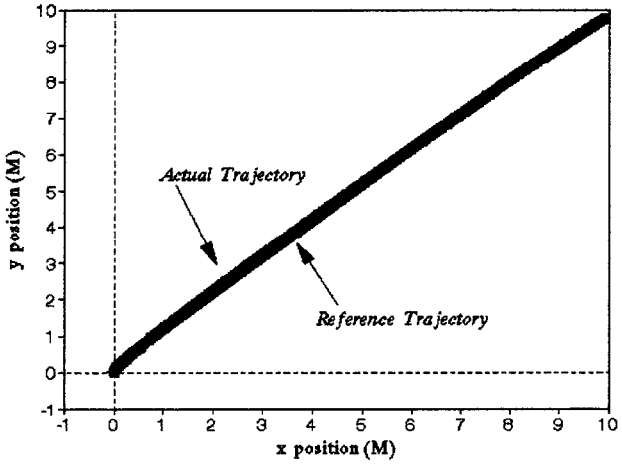

(c)

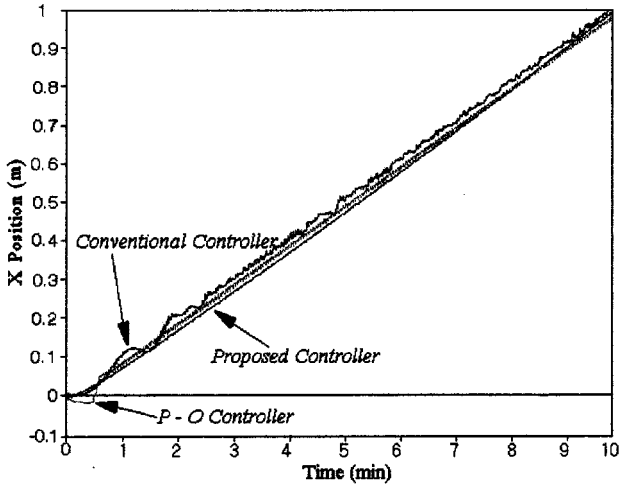

(d)

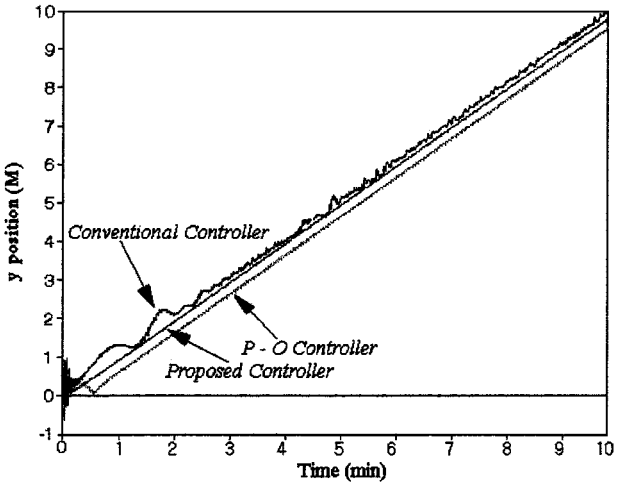

(e)

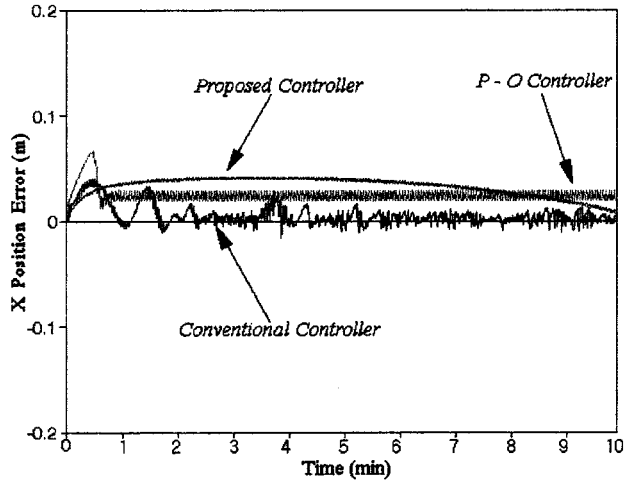

(f)

Fig. 8. Results using three feedback controllers in Figs. 4–6 for the diagonal reference trajectory. (a) Position solution trajectory of conventional system. (b) Position solution trajectory of position, orientation feedback system. (c) Position solution trajectory of proposed system. (d) Position solution trajectory for X axis. (e) Position solution trajectory for Y axis. (f) Position error trajectory for X axis.

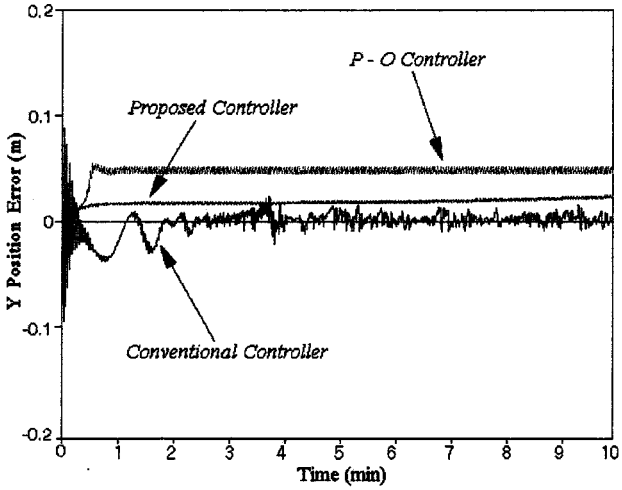

(g)

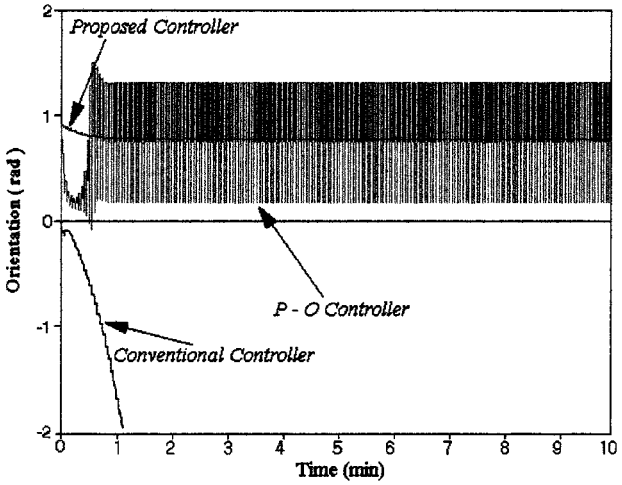

(h)

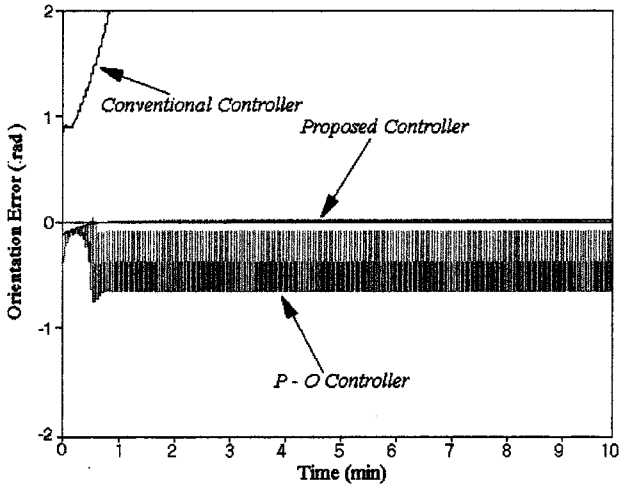

(i)

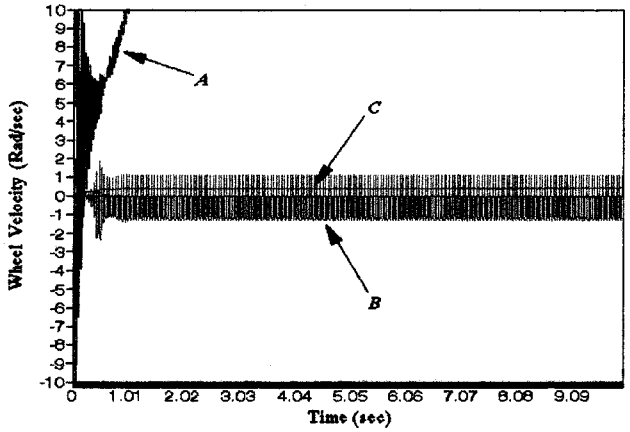

(j)

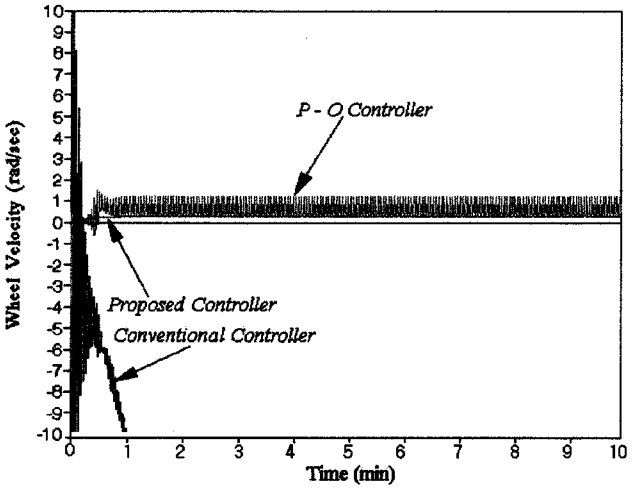

(k)

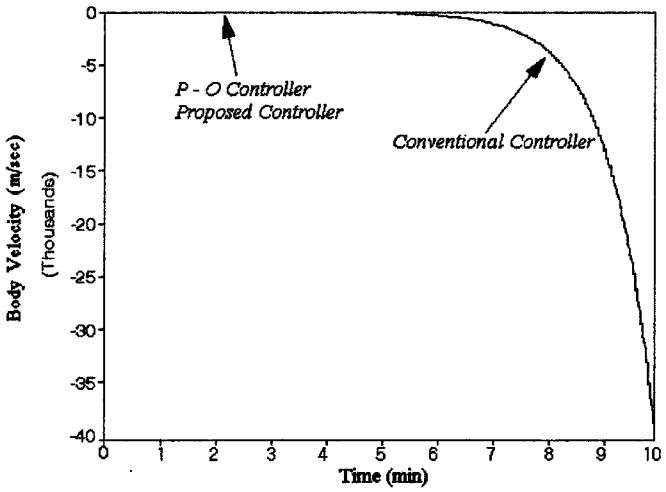

(l)

Fig. 8. *(Continued.)* Results using three feedback controllers in Figs. 4–6 for the diagonal reference trajectory. (g) Position error trajectory for Y axis. (h) Orientation solution trajectory. (i) Orientation error trajectory. (j) Velocity solution trajectory of wheel 1. (k) Velocity solution trajectory of wheel 2. (l) Body velocity for X axis. (m) Body velocity for Y axis.

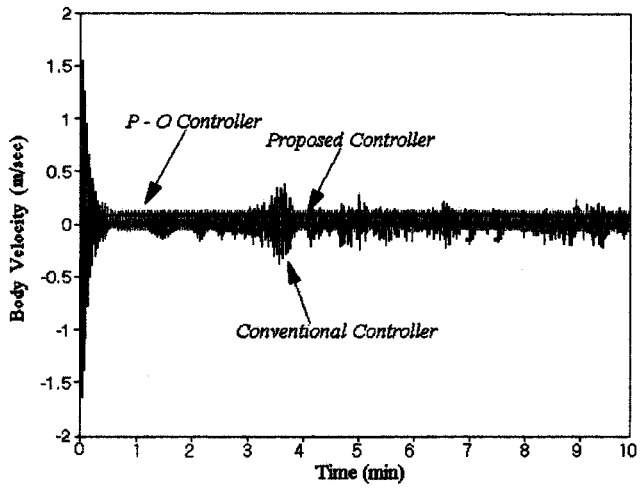

(m)

Fig. 8. *(Continued.)* Results using three feedback controllers in Figs. 4–6 for the diagonal reference trajectory. (m) Body velocity for Y axis.

velocity, and angular velocity, are obtained by multiplication of diagonal feedforward gain vector, as shown in (10) and (11)

$$ {}^{F}\dot{p}_B(nT) = K_p({}^{F}p_d(nT) - {}^{F}p_B(nT)) \tag{10} $$

$$ {}^{F}\dot{\theta}_B(nT) = K_o({}^{F}\theta_d(nT) - {}^{F}\theta_B(nT)). \tag{11} $$

Transformation to a surface coordinate system, from mobile robot velocity, is obtained by inverse motion matrix $M^{-1}(nT) = M^{T}(nT)$, and can be shown as (12)

$$ \begin{aligned} \begin{bmatrix} {}^{\overline{B}}\dot{p}_B \\ {}^{\overline{B}}\dot{\theta}_B \end{bmatrix} &= \begin{bmatrix} {}^{\overline{B}}v_{Bx} \\ {}^{\overline{B}}v_{By} \\ {}^{\overline{B}}\omega_{Bz} \end{bmatrix} \\ &= \begin{bmatrix} \cos{}^{F}\theta_B & \sin{}^{F}\theta_B & 0 \\ -\sin{}^{F}\theta_B & \cos{}^{F}\theta_B & 0 \\ 0 & 0 & 1 \end{bmatrix} \begin{bmatrix} {}^{F}v_{Bx} \\ {}^{F}v_{By} \\ {}^{F}\omega_{Bz} \end{bmatrix} \\ &= M^{-1} \begin{bmatrix} {}^{F}\dot{p}_B \\ {}^{F}\dot{\theta}_B \end{bmatrix}. \end{aligned} \tag{12} $$

The driving wheel's velocity can be obtained by a feedback algorithm, using kinematics shown in Fig. 5. It can be shown as (13)

$$ \begin{bmatrix} \omega_{w1x}(nt) \\ \omega_{w2x}(nt) \end{bmatrix} = \frac{1}{R} \begin{bmatrix} -S\theta & C\theta & l_a \\ -S\theta & C\theta & -l_a \end{bmatrix} \begin{bmatrix} {}^{F}\dot{p}_{eB}(nt) \\ {}^{F}\dot{\theta}_{eB}(nt) \end{bmatrix}. \tag{13} $$

The control algorithm, which uses each feedback compensating method for each wheel's position and orientation, is proposed to minimize internal error which occurs by inappropriate input of a time constant or loop gain.

C. Proposed Control System

In order to improve the tracking accuracy, we add a velocity feedback loop to the controller. The displacement difference between two driving wheels is turned into the velocity, and it goes to the driving wheel's velocity in order to compensate for orientation error. Conspicuous orientation error can be controlled by this technique. The orientation angle can be obtained as (14), through the two driving wheels' velocities which are sensed by encoders, and by the present orientation trajectory which is obtained from,

$$ \theta_t = \theta_{t-1} + \frac{R}{4l_a}\left(\left(\dot{q}_{1s(t-1)} + \dot{q}_{1s(t)}\right) - \left(\dot{q}_{2s(t-1)} + \dot{q}_{2s(t)}\right)\right). \tag{14} $$

Each wheel's driving distance can be calculated through each wheel's control loop gain $C1$, $C2$. Then, the difference of the two wheels' driving distance is as follows

$$ E(t) = |P_1(t)| - |P_2(t)|. \tag{15} $$

Here, a nonzero distance error $E(t)$ means that one wheel runs faster than the other wheel. The final configuration of the proposed controller is shown in Fig. 6. In this scheme, external error gains $C1$ and $C2$ are introduced to compensate for the error that occurs while the robot is moving along the curve. Tracking paths of the robot are classified as a linear path, and a round shaped path. While the robot moves along the circumference of radius D, in the round shaped path, two wheel velocities are derived as follows

$$ \dot{q}_1 = {}^{\overline{B}}\omega_{Bz}(D - l_a) = v(1 - l_a/D) \tag{16} $$

$$ \dot{q}_2 = {}^{\overline{B}}\omega_{Bz}(D + l_a) = v(1 + l_a/D) \tag{17} $$

where v is linear velocity of robot body, and ${}^{\overline{B}}\omega_{Bz}$ is robot angular velocity, while the robot is moving along a round shaped path. When the robot moves along the circular path, $C1$ and $C2$ are derived as (18) and (19) from (16) and (17)

$$ C1 = 1 \tag{18} $$

$$ C2 = \frac{\dot{q}_2}{\dot{q}_1} = \frac{1 + l_a/D}{1 - l_a/D}. \tag{19} $$

Linear motion occurs in one particular case. Then, $D = \infty$. If radius, $R1$, of the left wheel becomes bigger than radius, $R2$, of the right wheel (due to wearing of wheel circumference), the robot will make an ellipse trajectory; even though the two wheels' motor have the same torque. However, if $C1 = 1$ and $C2 = R1/R2$, then the error is compensated for. Each driving wheel's displacement difference can be derived from $C1 \times d_{w1}$ and $C2 \times d_{w2}$ respectively, which are multiplication of gain matrix $C1$ and $C2$. These gain matrices $C1$ and $C2$, are calculated under consideration of situations where the robot runs on a straight line or on a curved course. When the system is stable, and the reference trajectory is set up as a linear line without any disturbance, the difference of displacement is derived by selection of gain matrix, $C1 = C2 = 1$. However, in the case of the ellipse reference trajectory, gain matrix $C1$ and $C2$ are decided by (18) and (19). That is, the difference of displacement can be derived as (20), if the reference trajectory is a straight line

$$ E_{dw} = C1 \times d_{w1} - C2 \times d_{w2} = d_{w1} - d_{w2} \tag{20} $$

the definition of d_{w1}, d_{w2} is the driving distance of wheel 1 and 2, respectively.

TABLE II
X, Y AXES POSITION TRAJECTORY FOR THE SIMULATION

	Conventional Controller(A)		Position-orientation Controller (B)	Proposed Controller
X axis	Convergence rate	Continuous Vibration	Good	Very Good
	Convergence Time	2.87 sec	0.77 sec	0.001 sec
Y axis	Convergence rate	Continuous Vibration	Good	Very Good
	Convergence Time	2.75 sec	0.64 sec	0.012 sec

TABLE III
ORIENTATION TRAJECTORY FOR THE SIMULATION

	Conventional Controller (A)	Position-orientation Controller (B)	Proposed Controller (C)
Limit of Orientation	Continuously Decrease	1.34~0.23 rad	0.750 rad
Convergent Time	No Convergence	0.877 sec	0.002 sec

TABLE IV
BODY VELOCITY IN Y AXIS

	Conventional Controller (A)	Position-orientation Controller (B)	Proposed Controller (C)
Maximum Velocity	1.641 m/sec	0.232 m/sec	0.103 m/sec
Minimum Velocity	-1.695 m/sec	0.068 m/sec	0.092 m/sec

If the reference trajectory is a round shape with radius D, then the difference of displacement is derived as (21)

$$\begin{aligned} E_{dw} &= C1 \times d_{w1} - C2 \times d_{w2} \\ &= (q_{w1} \times 2.0 \times \pi \times R_1)/360 \\ &\quad - \frac{1 + l_a/D}{1 - l_a/D}(q_{w2} \times 2.0 \times \pi \times R_2)/360 \end{aligned} \quad (21)$$

where, $C1$ and $C2$ are gain matrices that might have different data, according to reference trajectory type. As a conclusion, the angular acceleration of each wheel of a WMR can be derived as (22), which has separated position and orientation feedback loops, with internal error compensator, and external error compensator.

The compensated velocity $\mathrm{CVW3}(t)$ is obtained by the proportional controller and the integral controller, using the displacement of each wheel. $\dot{q}_1$, $\dot{q}_2$ in Figs. 5 and 6 are defined as the driving wheels' angular velocity. It can be described by multiplying the driving wheel's radius, by the revolution speed for the X axis of the driving wheel together

$$\mathrm{CVW3}(t) = E_{dw}(t) * K3 + K4 \int_{(n-1)t}^{nt} E_{dw}\, dt. \quad (22)$$

TABLE V
COMPARISON OF TWO DRIVING WHEELS' VELOCITIES

Wheel radius	Average driving velocity of wheel 1	Average driving velocity of wheel 2	Remark
R1=0.11R2=0.11	0.288 rad/sec	0.285 rad/sec	Simulation A
R1=0.11R2=0.09	0.286 rad/sec	0.360 rad/sec	Simulation B

The result of (22) is supplied to each wheel with positive (+), or negative (−) value for compensation. It means that while the mobile robot moves on a straight line, the driving distance of wheel 1 is longer than that of wheel 2. Therefore, the driving velocity of wheel 1 should be decreased, while that of wheel 2 should be increased. For the four-wheeled two-degrees-of-freedom differential driving mobile robot, angular acceleration of each wheel can be described as (23), based on the position-orientation control system, and the external error compensation system that is designed to compensate for internal error

$$\begin{aligned} \begin{bmatrix} \dot{\omega}_{w1x}(nt) \\ \dot{\omega}_{w2x}(nt) \end{bmatrix} &= \left(J^{+} M \begin{bmatrix} -K_p({}^{F}P_{eB}(nt)) \\ -K_o({}^{F}\theta_{eB}(nt)) \end{bmatrix} \right. \\ &\quad \left. + \begin{bmatrix} -(d_{\omega l} * C1 - d_{w2} * C2) * K3 \\ +(d_{\omega l} * C1 - d_{w2} * C2) * K3 \end{bmatrix} \right) \\ &\quad - \begin{bmatrix} K_1 \dot{q}_{1s}(nt) \\ K_2 \dot{q}_{2s}(nt) \end{bmatrix}. \end{aligned} \quad (23)$$

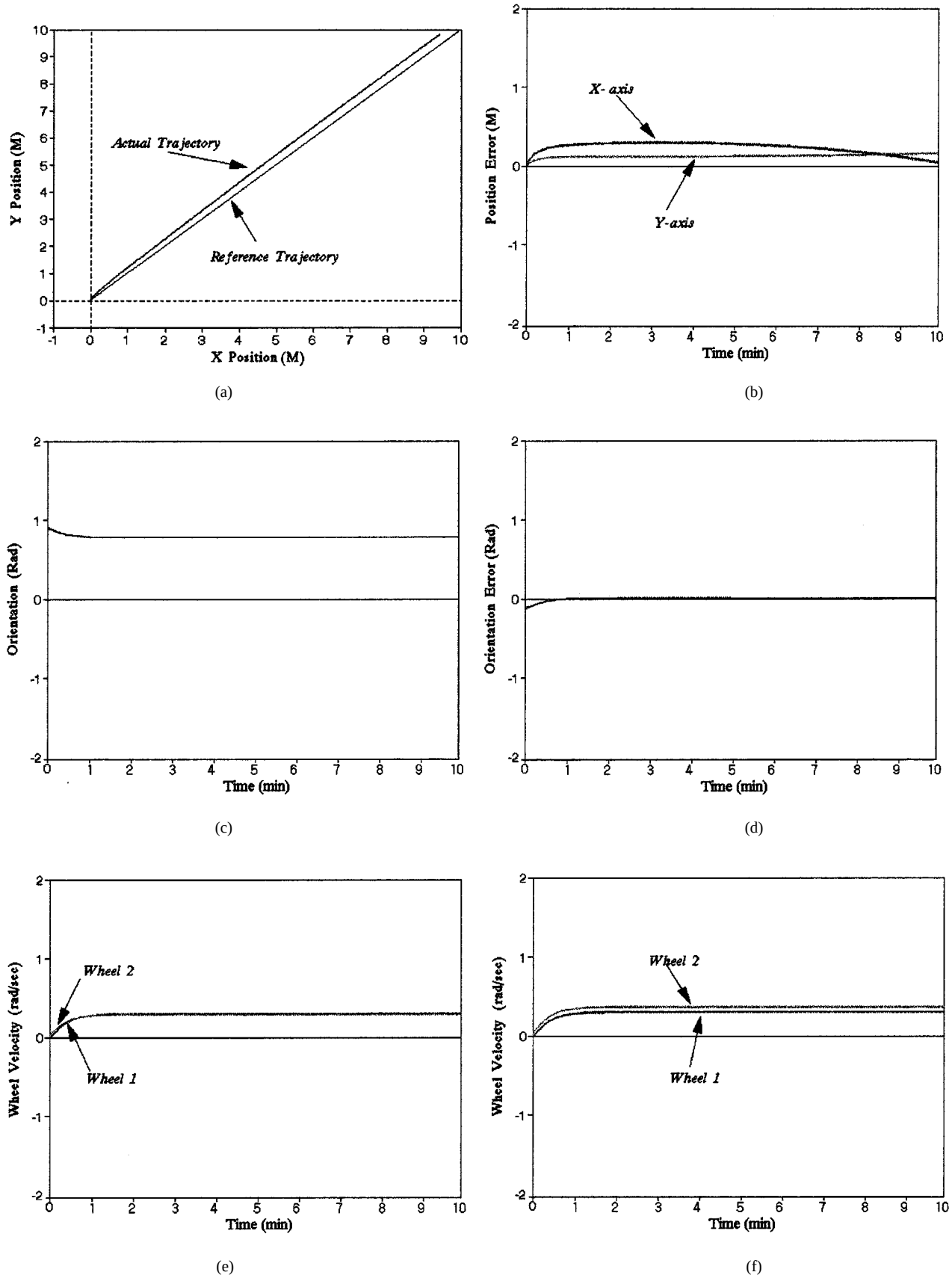

Fig. 9. Results of the driving wheel radius $R1 = 0.11$, $R2 = 0.09$ for proposed system. (a) Position solution trajectory. (b) Position error trajectory for X, Y axis. (c) Orientation solution trajectory. (d) Orientation error trajectory. (e) Velocity solution trajectory of wheel ($R1 = 0.11$, $R2 = 0.11$). (f) Velocity solution trajectory of wheel ($R1 = 0.11$, $R2 = 0.09$).

V. Computer Simulation and Results

To compare and evaluate the performance of our proposed kinematic's model, and control algorithm for mobile robots with the conventional counterpart, computer simulation is helpful. All of the feedback control systems used here, are based on systematic kinematic's modeling and dead-reckoning algorithm. In the simulation, the reference trajectory is described as robot body position trajectory for fixed surface coordinate. The real system to which we are going to apply the above algorithm is shown in Fig. 7. All parameters that are used in the computer simulation are also shown in Table I.

The reference trajectory which the WMR has to follow is set up as the diagonal line, (0,0)–(10,10), in Cartesian coordinates. The path tracking was tested by computer simulation and plotted for every 10 ms.

A. Path Tracking for Diagonal Line Reference Trajectory

When the reference trajectory is set up as a diagonal line, each control system's trajectory of position solution, in X, Y axis, trajectory of position error, trajectory of orientation solution, trajectory of orientation error, trajectory of each wheel's velocity solution, and trajectory of body velocity for each axis, are shown in Fig. 8. To compare the two control systems' performance, each output is shown in Tables II–IV.

Fig. 8(d) and (f) show position trajectory and position error trajectory for the X-axis of a 3-control system. The conventional control system pursues the reference trajectory with a big position error of 0–2 s. After that, small error continuously follows. The proposed control system smoothly pursues the reference trajectory in X-axis without big initial error or trajectory error.

Fig. 8(e) and (g) show trajectory of position and trajectory of position error in the Y-axis of a 3-control system. The conventional control system shows a big chattering error in the initial state and then converges with continuous small error. The position-orientation feedback control system has a continuous error of 0.56 m at 5.7 s and sustains error of 0.45, up to the final state. The proposed control system shows a continuously very small error of 0.19 m–0.23 m without any change.

The trajectory of orientation and orientation error of a 3 control system are shown in Fig. 8(h) and (i). Through the simulation result of a conventional system, we find that orientation trajectory has insignificant convergence to that of position trajectory, because the conventional control system uses only a gain, K, to minimize the error and a reference trajectory that has position and orientation together. However, if separated position and orientation reference are supplied as inputs, and the system has its own gains, Ko, Kp, then it has a faster convergence rate than that of the conventional system. However, it has continuous chattering within small range. The proposed control system has a uniform orientation trajectory error of 0.750 rad without chattering. Fig. 8(j) and (k) show the velocity profile of the WMR's driving wheel for three types of control systems. The two wheels' driving velocities in a conventional system do not have constant velocity, but positive or negative velocity tends to increase. The position-orientation feedback controls system keeps up the velocity that has arbitrary value in a limited range of positive and negative velocity. However, the proposed control system has nearly constant speed with 0.288 rad/s.

In Fig. 8(l) and (m), the WMR's body velocity profiles of three types of control systems for body coordinates are shown. The conventional system's body velocity for the Y-axis has large positive and negative amplitude at its starting point, and then sustains small amplitude continuously. The position-orientation feedback control system has arbitrary value, in a limited range of positive velocity and negative velocity. However, finally, the proposed system's velocity for the Y-axis is sustained with constant velocity of 0.103 m/s.

TABLE VI
Gains for Simulation (No Existence of External Error)

Reference trajectory	Conventional system	Position-orientation Feedback system	Proposed system
Straight line	K=90	Kp=20, Ko=14	Kp=4, Ko=3, PI=1, K1=1, K2=1, C1=1, C2=1

TABLE VII
Gains for Simulation (with Existence of External Error in Proposed Controller. That is Due to Difference Between Two Driving Wheel's Radius)

Radius of driving wheel	Kp	Ko	K1	K2	C1	C2
R1=0.11 R2=0.11	4	3	1	1	1	1
R1=0.11 R2=0.09	4	3	1	1	1	0.95
R1=0.11 R2=0.04	4	3	1	1	1	0.875

B. Simulation Result Analysis of Controller for External Error

When two driving wheels' radii are set up differently, as $R1 = 0.11$ and $R2 = 0.09$, external error occurs, and the proposed control system has a convergence (see Table V).

Fig. 9 shows the position tracking trajectory for gains $C1$ and $C2$, which were arranged where the two wheels don't have the same radius, due to unbalanced wear. It shows optimum trajectory tracking when $C1 = 1$, $C2 = 0.95$. In this case, position trajectory, orientation trajectory, position trajectory error and orientation error for X and Y axes are shown in Fig. 9(a)–(d). In the case where driving wheel radius $R1 = 0.11$ and $R2 = 0.11$, the velocity trajectories of the driving wheels are shown in Fig. 9(e). In the case when driving wheel radius $R1 = 0.11$, $R2 = 0.09$, velocity trajectories of the driving wheels are shown in Fig. 9(f). Through computer simulation, we find that the two driving wheels have almost the same velocities when they have the same radius, but velocity change appears when there is a different radius. Moreover, we also find that orientation trajectory tracking, for reference trajectory, is well achieved without the influence of wheel radius change.

The values of $K1$, $K2$, $K3$, and PI gains in Fig. 6 are optimal values that are chosen by the result of numerous partial computer simulations. However, varying the selection of reference trajectory such as straight line, curved line, and the occurrence of external error, will yield other optimal values.

The gains for each controller are as shown in Tables VI and VII.

VI. Conclusion

In this paper, we have proposed a kinematic's modeling and control algorithm that can follow a reference trajectory. We also tested the feasibility of the system by computer simulation. The kinematic's modeling was designed for a WMR that is driven and steered by two driving wheels. To determine the WMR position in real time, a dead-reckoning algorithm was added. Previous research into WMR control systems showed that external error, due to unexpected environmental situations, had hardly been considered. However, we separated the error into an internal error and external error, which made it possible to follow the desired trajectory more accurately. The feasibility of the control system, designed to compensate for the internal and the external error, was tested by computer simulation. The simulation showed that the system had fast and accurate position tracking, with remarkable diminishment of orientation error. However, the main problem with this kinematic's model and control algorithm is its complexity. In particular, the proposed control system is coupled together in the system elements in order to control the errors. So, simplification of the connections among the system elements are required.

For further study, we must pay more attention to developing the technique of giving a retouch and compensation when we apply it to a real system. Also, we have to work out new techniques in order to apply this algorithm to dynamic models.

References

[1] S. K. Shha and J. Angeles, "Kinematics and dynamics of three-wheeled 2-DOF AGV," in *Proc. IEEE Int. Conf. Robotics and Automation*, May 1989, pp. 1572–1577.

[2] P. Muir and C. Newman, "Kinematic modeling of wheeled mobile robots," *J. Robot. Syst.*, vol. 4, no. 2, pp. 281–333, 1987.

[3] P. P. Petrov, "Robust trajectory tracking algorithms for a wheeled mobile robot," in *Proc. IEEE IECON'91*, 1991, pp. 1071–1074.

[4] Y. Kanayama, "Two dimensional wheeled vehicle kinematics," in *Proc. IEEE Int. Conf. Robotics and Automation*, 1994, pp. 3079–3084.

[5] Y. Zhao and S. L. Bement, "Kinematics, dynamics and control of wheeled mobile robots," in *Proc. IEEE Int. Conf. Robotics and Automation*, May 1992, pp. 91–96.

[6] T. and H. F. Durrant, "Kinematics for modular wheeled mobile robots," in *Proc. IEEE Int. Conf. Robotics and Automation*, Apr. 1991, pp. 1130–1135.

[7] P. N. Sheth and J. J. Uicker, Jr., "A generalized symbolic notation for mechatronics," *J. Ind. Eng.*, vol. 93, no. 7019, pp. 102–112, 1971.

[8] J. J. Craig, *Introduction to Robotics: Mechanics & Control*. Reading, MA: Addison-Wesley, 1986.

[9] T. Burke and F. Durrant-Whyte, "Kinematics for modular wheeled mobile robots," in *Proc. IEEE/RJS Int. Conf. Intelligent Robots and System*, July 1993, pp. 1279–1286.

[10] B. Steer, "Trajectory planning for a mobile robot," *Int. J. Robot. Res.*, vol. 8, no. 5, pp. 3–14, Oct. 1989.

Yongoug Chung was born in Chinju, Korea, in 1969. He received the B.S., M.S., and Ph.D. degrees in electronic engineering from Kyung Hee University, Seoul, Korea, in 1988, 1992, and 1998, respectively.

He is currently an Assistant Professor in the School of Automotive Engineering, Chinju College, Chinju City, Korea. His primary areas of interest are mobile robots, force/position control of robot manipulators, and mechatronics.

Chongkug Park (M'89) was born in Korea in 1945. He received the B.S. degree in physics from Seoul National University, Seoul, Korea, and the M.S. and Ph.D. degrees in electrical engineering from Yonsei University, Seoul, Korea, in 1971, 1975, and 1979, respectively.

From 1987 to 1988, he was a Visiting Professor at Oregon State University. From 1995 to 1998, he was Associate Dean of the Graduate School of Industry and Information, Kyung Hee University, Yongin-Shi, Korea, where he is currently a Professor and Dean, College of Engineering. His research interests include robotics, mechatronics, fuzzy logic, and neural networks.

Prof. Park was President of the Korean Fuzzy Logic and Intelligent Systems Society (KFIS) from 1998 to 1999. He received the Academic Achievement Award from the Korea Institute of Electrical Engineers in 1979 and Distinguished Service Awards from the Institute of Electronics Engineers in Korea and KFIS in 1996 and 2000, respectively. He was a Member of the Board of Directors of the Society of Instrument and Control Engineers of Japan from 1999 to 2000.

Fumio Harashima (M'75–SM'81–F'88) was born in Tokyo, Japan, in 1940. He received the B.S., M.S., and Ph.D. degrees in electrical engineering from The University of Tokyo, Tokyo, Japan, in 1962, 1964, and 1967, respectively.

He was an Associate Professor in the Institute of Industrial Science, University of Tokyo, in 1967, and a Professor from 1980 through 1998. He was Director of the Institute from 1997 to 1995. In 1996, he joined Kagawa University as an Adjunct Professor for the purpose of establishing a new faculty of engineering, which opened in April 1998. He has been President of Tokyo Metropolitan Institute of Technology, Tokyo, Japan, since April 1998. His research interests are power electronics, mechatronics, and robotics. He is the coauthor of four books and has authored more than 1000 published technical papers. He has been active in various academic societies, such as the Institute of Electrical Engineers of Japan (IEEJ), Society of Instrument and control Engineers of Japan (SICE), and Robotics Society of Japan.

Dr. Harashima served as President of the IEEE Industrial Electronics Society (IES) in 1986–1987 and as Secretary in 1990. He was also a Member of the IEEE N&A Committee in 1991–1992 and IEEE Fellow Committee in 1991–1993. He served as Editor-in-Chief of the IEEE/ASME TRANSACTIONS ON MECHATRONICS in 1995. He has received a number of awards, including the 1978 SICE Best Paper Award, 1983 IEEJ Best Paper Award, 1984 IES Anthony J. Hornfeck Award, and 1988 IES Eugene Mittelmann Award. He is a Fellow of SICE.